Chapter 6: Molecular Thermochromic Materials

Synthesis and Studies on Thermochromic Compounds A_2CuCl_4 : [(naphthyl ethylamine)$_2$CuCl$_4$]

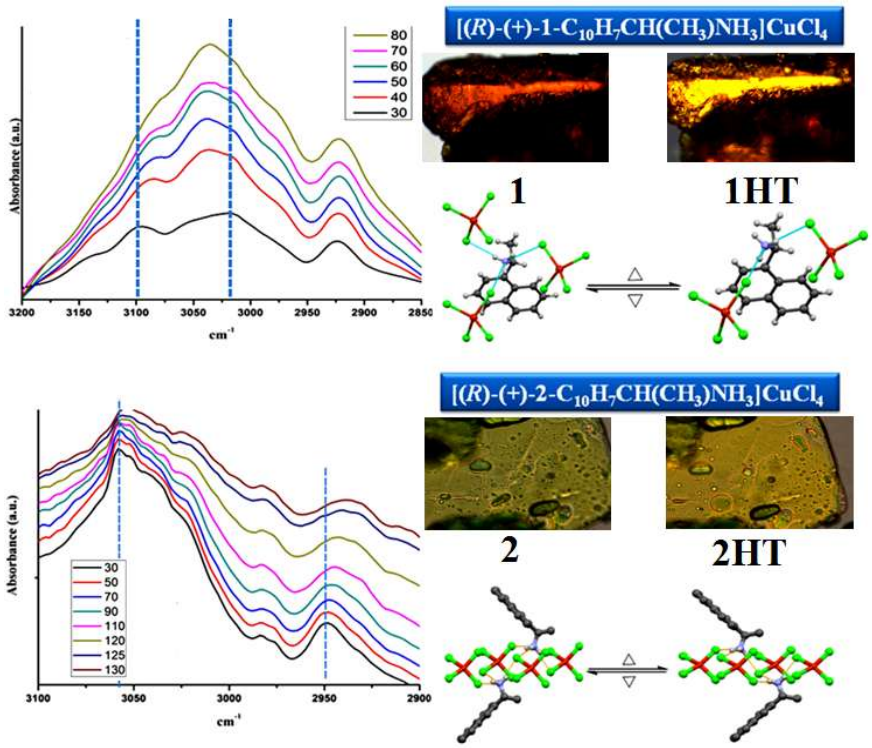

Chromogenic materials are those compounds which shows reversible change in color/ optical properties in visible region when subjected to change in their surroundings such as heat, pressure, light and electrons. There are four major types of chromogenic materials – photochromic (PC), electrochromic (EC), piezochromic (PEC) and thermochromic (TC). Photochromic effect (PC) occur due to irradiation by light (photons), electrochromic effect (EC) due to an applied electric field, piezochromic (PEC) due to application of pressure and thermochromic effect (TC) due to change in temperature. Here we are interested in thermochromic material that changes colour upon thermal stress in a wide range of materials, ranging from organic [1] to inorganic [2], in solid or liquid state [3] involving emission [4] and/or absorption behavior. It is the simplest way to detect solid-state phase transitions in which the color of the crystals change with change in temperature. Thermochromism with phase transitions can be classified in two classes**.** Continuous thermochromism is a gradual change in crystal color and is of a first order type phase transition, whereas discontinuous thermochromic phase transition is evidenced by a remarkable change in crystal color at critical temperature and is indicative of a sudden change in crystal properties at that temperature [5].

Thermochromism having wide range for technical applications e.g. thermometers, thermoplastics, duroplastics, gels, coating powder and temperature sensors. It also occurs in inorganic materials such as oxides (vanadium oxide and zinc oxide) [6] and metal complexes/salts (Cuprous mercury iodide, Cu_2HgI_4) which can be easily prepared and showing reversible transitions at quite low temperatures [7], in liquid crystals [8], in conjugated oligomers [9] and in leuco dyes [10]. The reversible color change are due to change in their crystal structure with temperature [11]. Mostly thermochromic dyes are organic compounds which showed irreversible colour change with temperature.

Our Interest: Designing and synthesizing new 'set of thermochromic molecules' and understanding their opto-structural correlations.

Abstract:

In this chapter, we have synthesized two new copper based compounds with a general formula $(R\text{-}NH_3)_2CuCl_4$, [where, $R\text{-}NH_3$ = *(R)*-(+)-napthyl-1-ethylamine **(3)** and *(R)*-(+)-2-napthyl-1-ethylamine **(4).** These compounds were investigated using thermal analyses (TG-DTA and DSC), polarizing microscope and single crystal XRD spectroscopy. DSC measurement and polarizing microscope images showed reversible solid-solid phase transitions at HT leading to thermochromic behavior. Compound **3** showed solid-solid phase transitions at LT also, but without thermochromic effect.

Single crystal XRD studied on these compounds revealed that both compounds crystallized in the chiral polar space group. Compound **3** crystallized in chiral monoclinic space group $P2_1$ with cell dimensions a = 12.7159(4) Å, b = 7.1977 (2) Å, c = 14.0548 (4) Å, β = 94.371 (2) °, V = 1282.63(7) $Å^3$ and Z = 2. Compound **4** is crystallized in monoclinic space group *C*2, chiral (polar) space group, with unit cell dimensions a=10.7967(3) Å, b = 7.2349(2) Å, c = 16.9456(4) Å, β = 97.004(2)°, V = 1313.79(6) $Å^3$ and Z = 2.

Single crystal and temperature dependent FT-IR study revealed unique synthons and motifs for NH···Cl hydrogen bonding are responsible for the observed phase transition and thermochromic behavior.

6.1 Introduction

Organoammonium tetrachlorocuprates (II) (A_2CuCl_4, where A= organic amine) have been known to undergo reversible change in color at different temperatures in the solid state [12]. It is observed that, thermochromism in these A_2CuCl_4 based compounds is driven by the change in geometry around $CuCl_4^{2-}$ anion (Scheme 6.1). Geometry around Cu^{2+} and color can be correlated by the average *trans* angle. The $CuCl_4^{2-}$ ion shows average *trans* Cl-Cu-Cl angle around 180º for green coloured square planar complexes and 109.58° for blue/red coloured tetrahedral complexes. In case of distorted tetrahedral geometry, it exhibits yellow/green color, normally at room temperature, when the *trans* angle is ~140º. The color change to deeper green with increase in *trans* angle and towards orange as the angle decrease [13].

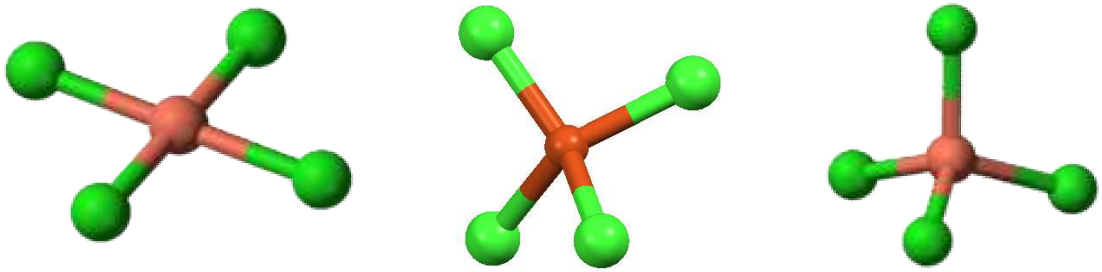

Square planar Distorted Tetrahedral Tetrahedral

Scheme 6.1: Different geometries of $CuCl_4^{2-}$ ion

Due to Jahn-Teller effect, $CuCl_4^{2-}$ ion does not have a regular tetrahedral geometry but has predominant compressed tetrahedron geometry. However, it is also possible for $CuCl_4^{2-}$ ion to adopt a centrosymmetric square planar geometry with *D*4h symmetry. To achieve square planar geometry for $CuCl_4^{2-}$ anion counter cation, primary amine, should be large and bulky. Till date there have been only five compounds reported with the square planar geometry compared with the large number of reported distorted tetrahedral complexes [14]. A problem with bulky cation structure is that they will destabilize a typical two-dimensional layered structure and consequently structural phase transitions. Therefore addition of non-covalent bondings, such as hydrogen bonding might prove useful.

The most common synthons observed in A_2CuCl_4 commpounds are due to NH···Cl interaction are shown in scheme 6.2. To our best knowledge, we present first time relation between thermochromism and different NH···Cl synthons or motifs [15].

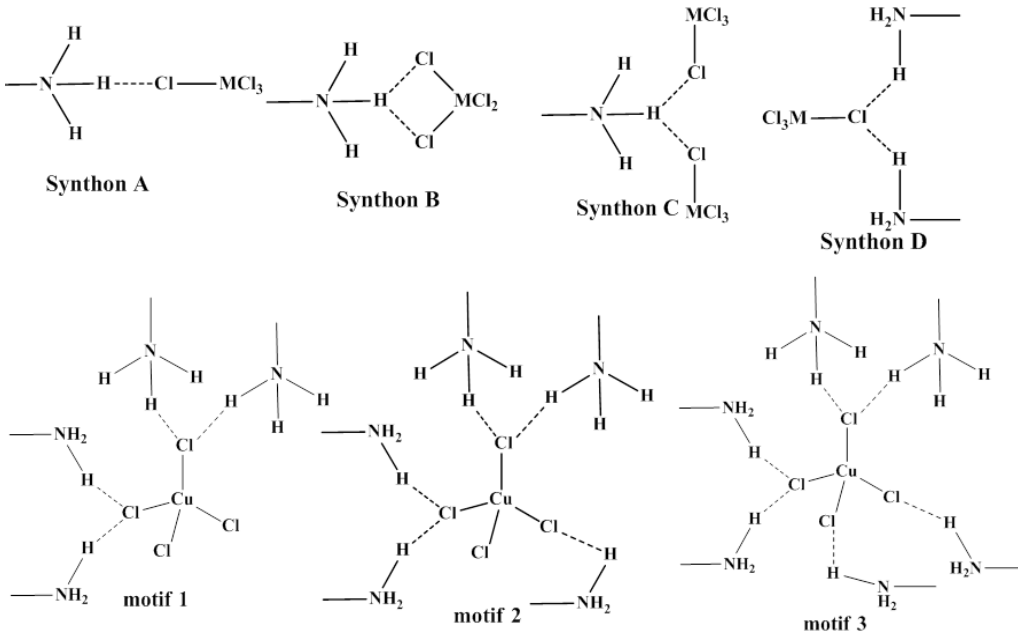

Scheme 6.2: Types of different synthons and motifs

We report here use of rigid regioisomeric ligands- (*R)*-(+)-napthyl-1-ethylamine (**1**) and (*R)*-(+)-2-napthyl-1-ethylamine (**2**). Bulky cations was used to minimize distortion of the $CuCl_4^{2-}$ ion geometry during phase transitions and to observe ligand centric thermochromism. In this aspect, we observed presence of Cl···NH supramolecular synthons controls the crystal structures (Synthon A, Synthon B, Synthon C and Synthon D) and play coherent role in a designed manner [16], [17], [18]. We confirm our understanding using single crystal X-ray, DSC, temperature dependant FT-IR and photoluminescence measurements.

Motivation: Thermochromism is a change in color upon thermal stress. It occurs due to changes in co-ordination sphere around a metal center or by ligands movement. We sought to study latter effect, molecular in origin, by employing rigid regio-isomeric ligands.

6.2 Experimental

6.2.1 Materials and Methods:

All chemicals and solvents were of analytical grade reagents. (*R)*-(+)-napthyl-1-ethylamine **(1)**, (*R)*-(+)-2-napthyl-1-ethylamine **(2)** and copper (II) chloride were from Aldrich; conc. Hydrochloric acid (Qualigens) and ethyl alcohol (Baroda chemicals) were used without further purification.

6.2.2 Syntheses of compounds:

A general methodology of preparation/syntheses is mentioned in scheme-6.3.

Scheme: 6.3

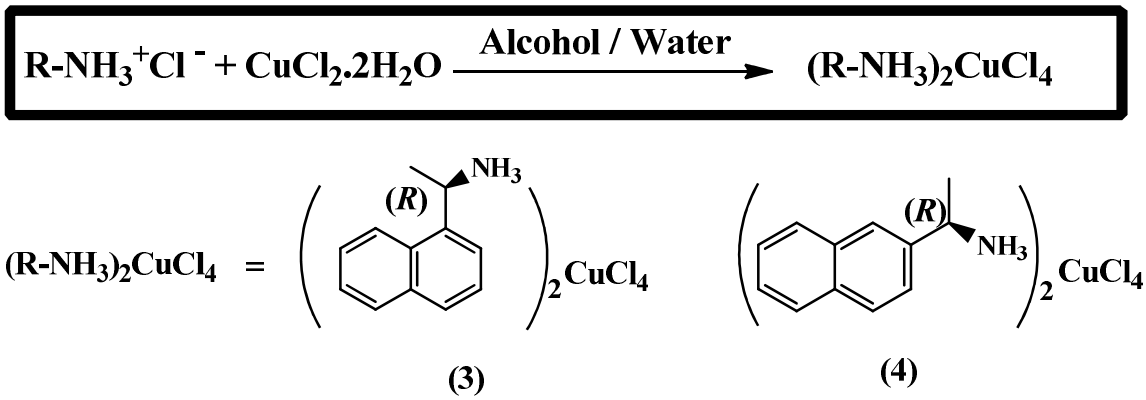

An acidified ethanolic solution (10 mL) containing (*R)*-(+)-napthyl-1-ethylamine/ (*R)*-(+)-2-napthyl-1-ethylamine (0.1 mmol) and copper (II)chloride (0.1 mmol) were mixed and refluxed for three hours. The resulting dark-green coloured solution was evaporated to dryness and washed with ether. It was then recrystallized using 2-3 ml ethanol. Yellowish orange (**3**) and green plate (**4**) -shaped crystals suitable for X-ray diffraction were obtained by slow evaporation of the solvents within 1 week.

Yield: 60-80%.

6.3 Result and Discussions

6.3.1 FT-IR:

Figure 6.1 shows the FT-IR spectra of compound **3** ((*R*)-(+)-1-$C_{10}H_7CH(CH_3)NH_3)CuCl_4$ and compound **4** ((*R*)-(+)-2-$C_{10}H_7CH(CH_3)NH_3)CuCl_4$ crystals respectively at RT.

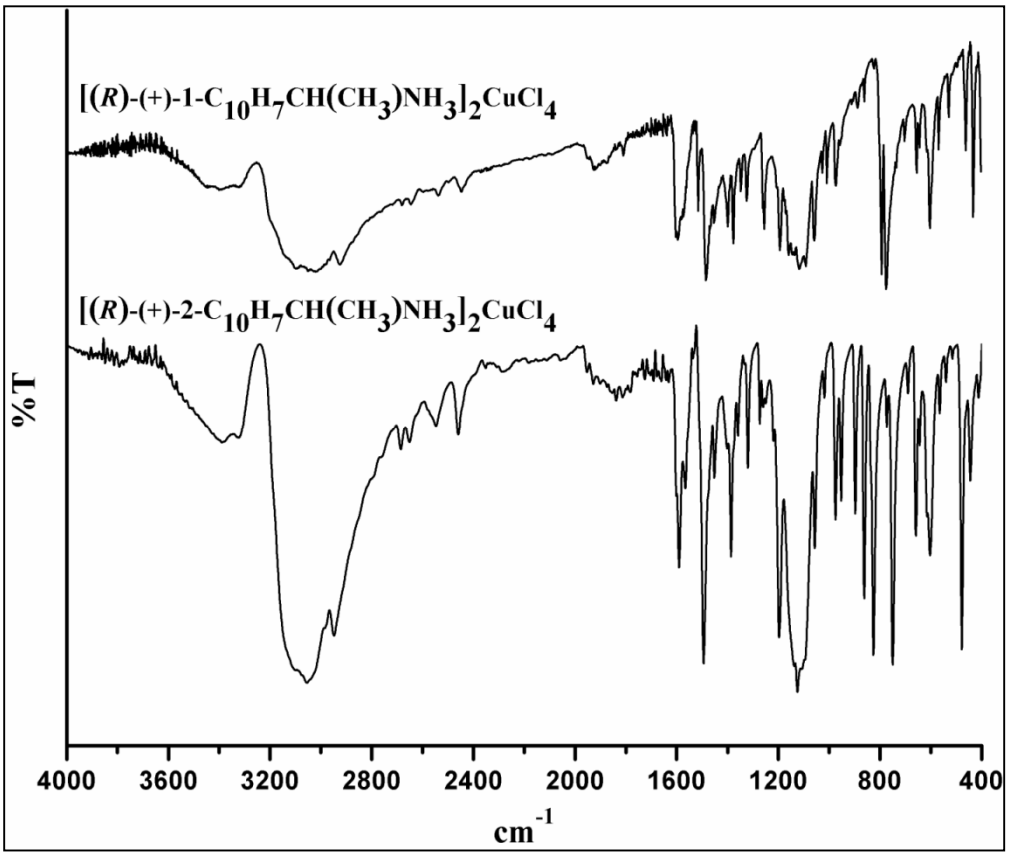

Fig. 6.1: FT-IR spectra of [(R)-(+)-1-$C_{10}H_7CH(CH_3)NH_3$]$CuCl_4$ (3) and [(R)-(+)-2-$C_{10}H_7CH(CH_3)NH_3$]$CuCl_4$ (4)

Compound 3- FT-IR (KBr): 3099 (m), 3028 (vs), 2923 (vs), 2678 (m), 2647 (m), 2537 (m), 2446 (m), 1807 (m), 1595 (vs), 1571 (s), 1515 (s), 1486 (vs), 1454 (s), 1400 (s), 1378 (vs), 1346 (s), 1322 (vs), 1262 (m), 1256 (vs), 1207 (m), 1194 (vs), 1178 (m), 1170 (m), 1159 (s), 1146 (m), 1137 (m), 1118 (s), 1091 (s), 1059 (vs), 1028 (s), 1010 (vs), 974 (vs), 958 (m), 887(s), 862 (m), 824 (m), 792 (vs), 775 (vssh), 737 (m), 703 (m), 656 (s), 663 (s), 616 (m), 604 (vssh), 569 (s), 530 (s), 462 (vs), and 433 (vs) cm^{-1}.

Compound 4- FT-IR (KBr): 3102 (m), 3057 (vs), 2948 (vs), 2689 (m), 2648 (m), 2544 (m), 2457 (s), 1603 (w), 1591 (vs), 1566 (s), 1533 (w), 1492 (vs), 1474 (m), 1400 (s), 1451 (s), 1401 (w), 1385 (vs), 1374 (w), 1357 (m), 1317 (vs), 1272 (m), 1259 (m), 1252 (m) 1218 (w), 1196 (vs), 1155 (m), 1137 (m), 1124 (s), 1118 (s), 1104 (w), 1094 (m), 1056 (vs), 1017 (s), 974 (vs), 951 (vs), 898 (vs), 860 (vssh), 827 (vssh), 773 (m), 748 (vssh), 689 (m), 659 (s), 644 (m), 613 (w), 603 (vs), 563 (m), 540 ms), 516 (w), 478 (vs), 443 (s) and 412 (m) cm^{-1}.

It is observed that stretching vibration bands of NH_3^+ present at 3028-3055 cm^{-1}. This region is also responsible for distinct signature of motifs formed due to N-H···Cl hydrogen bonds. Band at 2925 and 2949 cm^{-1} indicates the asymmetric stretching due to terminal methyl ($-CH_3$) group. The two sharp bands at 2682-2694 and 2647-2653 cm^{-1} attribute to Fermi resonance corresponding to combination bands of N-H ($-NH_3^+$) deformation modes and rocking modes. Other deformation modes were observed at 1051-1056 cm^{-1}. Bending modes of N-H were observed at 1592-1596 cm^{-1} while of C-H was observed at 1479-1494 cm^{-1}.

The other bands are assigned to the naphthalene ring [19]. The C-C stretching (weak) of the naphthalene ring was observed in the range of 1010-1017 cm^{-1} and at 1454 cm^{-1}. C-H bending was observed in the range of 1118-1137 cm^{-1}. Band at 1208 cm^{-1} was assigned to the C-H bend (-) at β position, C-C stretching, to and fro vibration of C3-C4 band in **3.** On the other hand in **4**, C-H bend (-) at α position, C-C stretching, to and fro vibration of C3-C4 band occurs at 1272 cm^{-1}. The C=C stretching is observed in the range of 1590-1597 cm^{-1}.

The strong band for C-H stretch (out of phase) was observed at 3037-3057 cm^{-1}. The medium bands at 615-617 cm^{-1} attributed to the CCC bend in two rings. Sharp bands were observed at 462 and 478 cm^{-1} for **3** and **4** were assigned to the CC-t: ring def (t-torsion, def- deformation). C-H wagging was observed at 774 cm^{-1} and at a range of 953-955 cm^{-1} with intense sharp peak.

6.3.2 Elemental analyses:

The calculated elemental analyses were consistent with the observed formulae of complexes.

Compound 3: Anal. Calc. for C_{24} H_{28} Cl_4 Cu N_2**:** C, 40.79; H, 4.67; N, 5.95%. **Found:** C, 41.1; H, 4.41; N, 5.78%.

Compound 4:Anal. Calc. for C_{24} H_{28} Cl_4 Cu N_2**:** C, 40.79; H, 4.67; N, 5.95%. **Found:** C, 40.6; H, 4.45; N, 5.69%.

6.4 Thermal Studies

6.4.1 TG-DTA:

Thermo-gravimetric studies were carried out for the complexes **3** and **4** in nitrogen atmosphere in the 303-823 K temperature range (Figure 6.2 a-b). The multistep decomposition pattern of **3** and **4** are very similar.

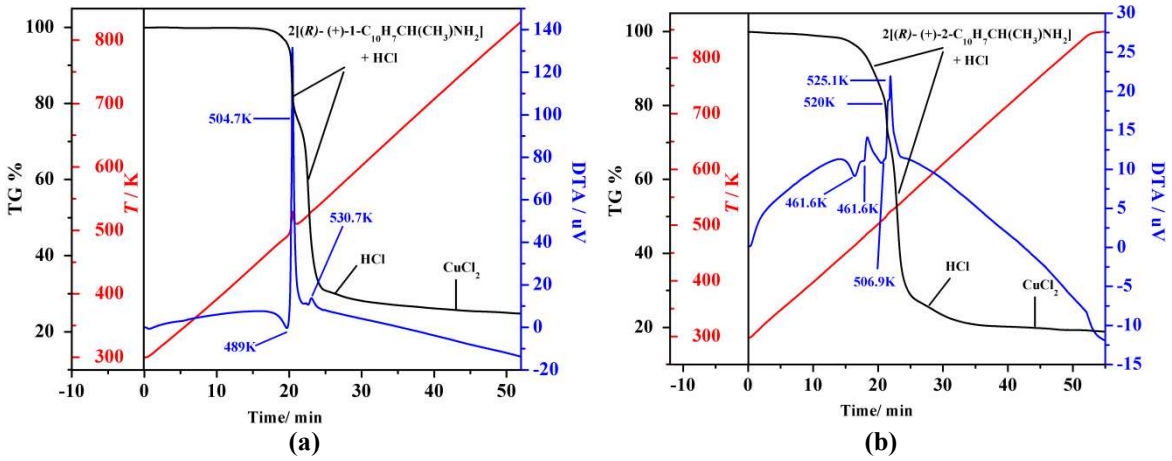

Fig. 6.2: TG/DTA thermogram for compounds 3 (a) and 4 (b)

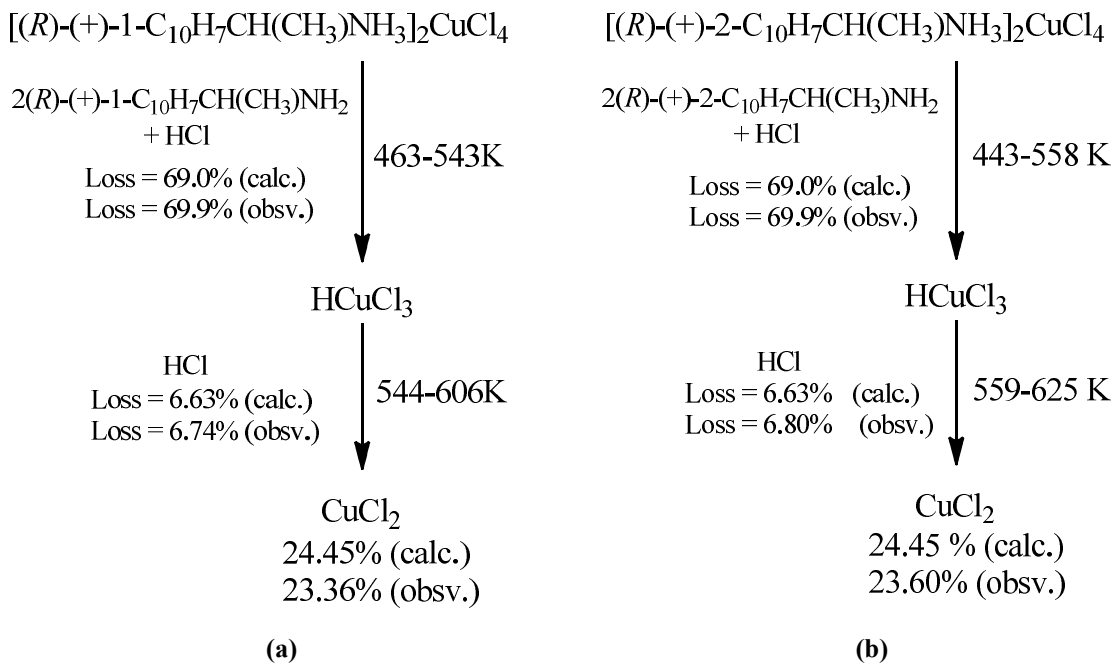

Fig. 6.3: Degradation pathway for compounds 3 (a) and 4 (b)

Complex **3** and **4** are stable up to 463 K and 443 K respectively, and then both organic ligands with single HCl molecule, decomposes gradually in the range of 463-543 K for **3** (Obsd. 69.9%, Calcd. 69%) and 443-558 K for **4** (Obsd. 69.6%, Calcd. 69%), followed by the one molecule of HCl (for **3** -Obsd. 6.74 %, Calcd. 6.63 % and for **4**- Obsd. 6.8 %, Calcd. 6.63 %). The remaining product at high temp is probable $CuCl_2$ (for **3**- Obsd. 23.36 %, Calcd. 24.45 %) and (for **4**- Obsd. 23.6 %, Calcd. 24.45 %) (Figure 6.3 a-b).

The DTA curves indicate that the decomposition of the compound took place with one endothermic peak at 489 K for **3** and two endothermic peak at 478 K for **4** along with phase transition at 461.6 K and 469.3K in case of **4** (Figure 6.2-a,b). Two small endothermic peaks in **4** which are too small for possible major structural change in the crystal. Two exothermic transitions responsible for crystallization, and desolvation/dehydration, were observed at 504.7 K and 530.7 K for **3** and 520 K and 525.1 K for **4**.

6.4.2 DSC:

To confirm the degradation pathways and exo-endothermic behavior observed in DTA, DSC study on these compounds were carried out (Figure 6.4). The DSC thermogram of compounds **3** and **4** confirms that these compounds be nonsolvated, as the thermogram shows a single thermally induced endothermic transition (solid- solid phase transition).

During heating, compound **3** and **4** shows single endothermic peak at 346.25K (-2.84 Jg^{-1}) and 397K (-13.60 Jg^{-1}) respectively while during cooling the only compound **4** shows the single exothermic peak at 371.06K (-1.92 Jg^{-1}). The compound **3** at low temperature shows single exothermic peak at 270K (-3.17 Jg^{-1}) during cooling and endothermic peak at 264.42K (7.05Jg^{-1}) during heating. These observed transitions are characteristics of the solid-solid phase transition.

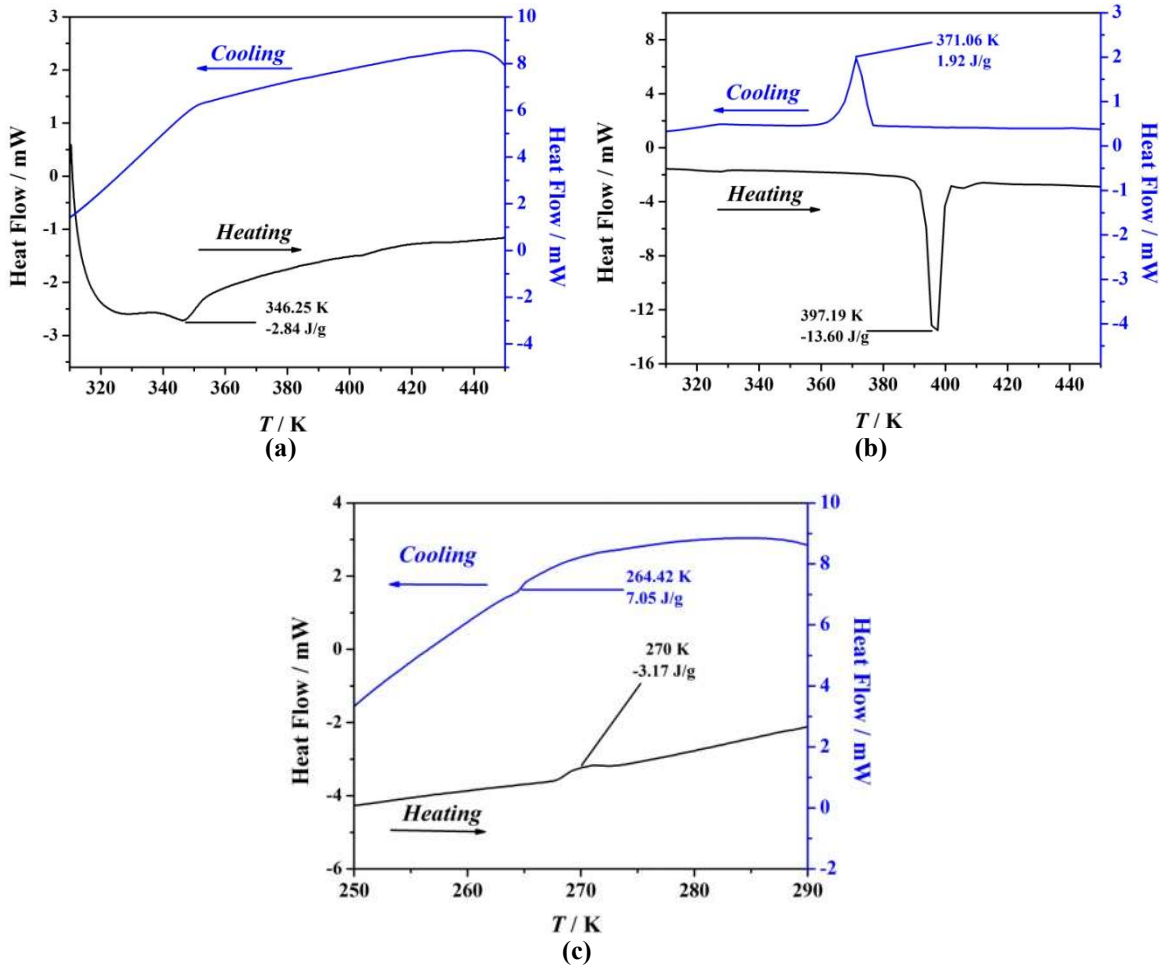

Fig. 6.4: DSC measurement plots for compounds 3(a), 4(b) at 300-450K and 3LT(c) at 200-300K

Table 6.1: DSC chart of compound 3, 3LT and 4 at different temperatures

Compounds	Phase Transition			
	Heating		Cooling	
	Temperature [K]	Enthalpy [Jg^{-1}]	Temperature [K]	Enthalpy [Jg^{-1}]
3	346.25	-2.84	No Transition	
3LT	270.00	-3.17	264.42	7.05
4	397.19	-13.60	371.06	1.92

To confirm these phase transition compounds were analyzed using a polarizing microscope (Figures 6.5-6.6). The polarizing microscope images show thermochromic behavior near phase transition temperature.

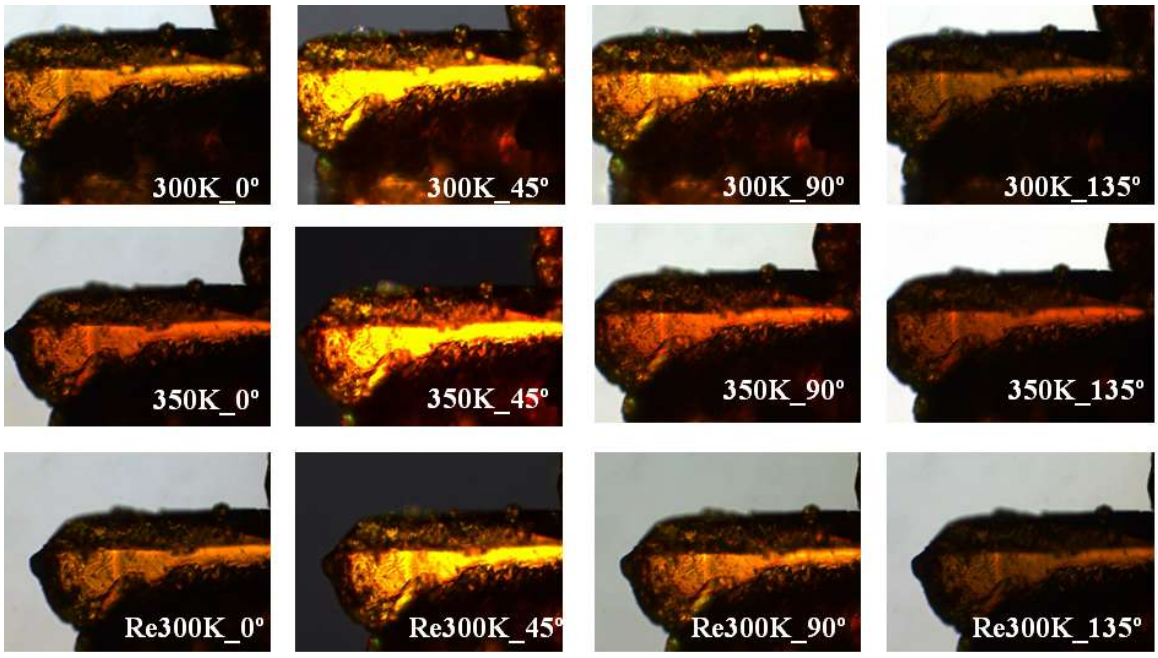

Fig. 6.5: Thermochromic behavior for compound 3 using polarizing microscope

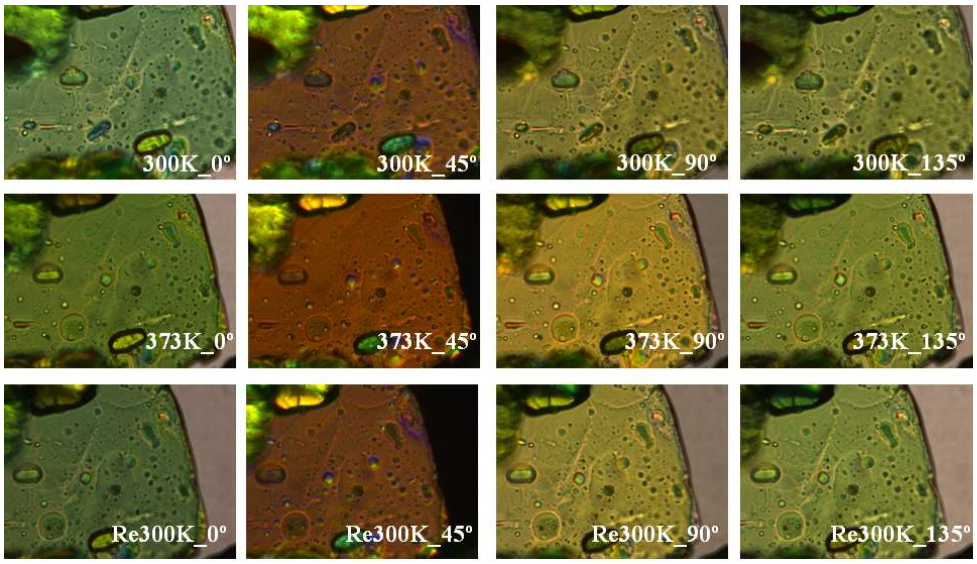

Fig. 6.6: Thermochromic behavior for compound 4 using polarizing microscope

The compound **3** shows Yellowish orange ↔ Red while compound **4** shows the Green yellow ↔ Brown color change confirms thermochromic nature.

6.5 Crystal structure: Single Crystal X-ray Diffraction

6.5.1 Crystal structure of 3 and 4 at 298K

Single crystal XRD confirms the formation of compounds and crystals. The molecular structure of **3** and **4** are shown in Figure 6.7.

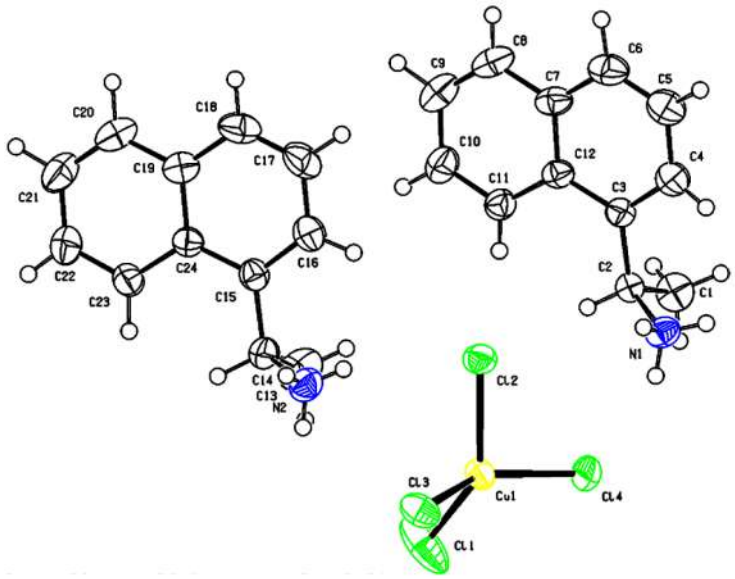

(a)

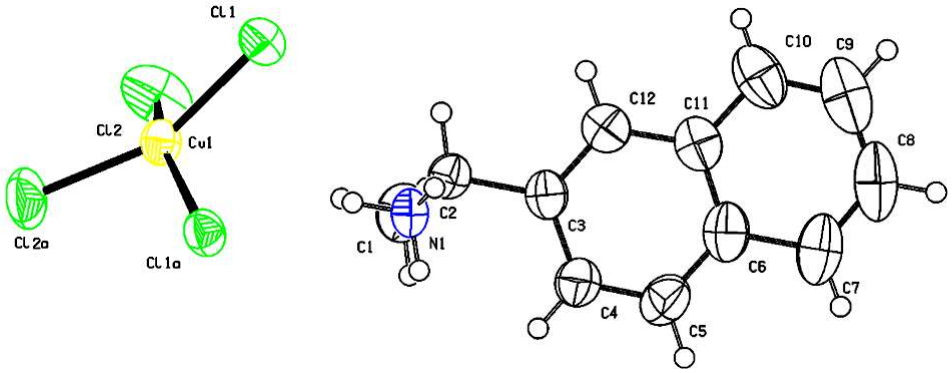

(b)

Fig. 6.7: Representation of the ellipsoid of thermal mean square displacements of non-hydrogen atoms at 50% of the asymmetric unit of (a) compound 3 and (b) compound 4

Table 6.2: Crystallographic data and structure refinements for compounds 3 and 4 at RT; at HT (3HT, 4HT) and at LT (3LT)

	3	3LT	3HT	4	4HT
Empirical formula	$C_{24}H_{28}Cl_4Cu\ N_2$	$C_{24}H_{28}Cl_4Cu\ N_2$	$C_{24}H_{28}Cl_4Cu\ N_2$	$C_{24}H_{28}Cl_4Cu\ N_2$	$C_{24}H_{28}Cl_4Cu\ N_2$
Formula weight	549.82	549.82	549.82	549.82	549.82
Temperature/K	296K	150K	350K	296K	373K
Wavelength	0.71073 Å	0.71073 Å	0.71073 Å	0.71073 Å	1.5418 Å
Crystal system	Monoclinic	Monoclinic	Monoclinic	Monoclinic	Monoclinic
Space group	$P2_1$	$P2_1$	$P2_1$	C_2	$P2_1$
Unit cell dimensions	a =12.7159(4)Å b = 7.1977 (2)Å c =14.0548(4)Å β = 94.371(2)°	a =12.6025(2)Å b = 7.1560 (1)Å c =13.9720(2)Å β = 94.340(1)°	a = 2.7730(9)Å b = 7.2107(5)Å c =14.0944(9)Å β = 94.344(6)°	a =10.7967(3)Å b = 7.2349(2) Å c =16.9456(4)Å β= 97.004(2)°	a =10.940(11)Å b = 7.2622(6)Å c =17.012(14)Å β= 96.877(9)°
Volume	1282.63(7) $Å^3$	1256.43(3) $Å^3$	1294.40(15) $Å^3$	1313.79(6) $Å^3$	1341.9(2) $Å^3$
Z	2	2	2	2	2
Density (calculated)	1.424 Mg/m^3	1.453 Mg/m^3	0.311 Mg/m^3	1.390 Mg/m^3	1.361 Mg/m^3
Absorption coefficient	1.282 mm^{-1}	1.309 mm^{-1}	1.021 mm^{-1}	1.252 mm^{-1}	1.138 mm^{-1}
Reflections collected	23355	16313	4091	7866	2063
Independent reflections	9585 [R(int) = 0.0217]	9128 [R(int) = 0.0149]	3052 [R_{int} = 0.0430]	4971 [R(int) = 0.0236]	1767 [R_{int} = 0.0468]
Refinement method	Full-matrix least-squares on F^2	Full-matrix least-squares on F^2	Full-matrix least-squares on F^2	Full-matrix least-squares on F^2	Full-matrix least-squares on F^2
Data / restraints / parameters	9585 / 1 / 392	9128 / 1 / 392	3052/26/285	4971/1/141	1767/27/119
Goodness-of-fit on F2	1.047	1.003	1.105	1.002	1.363
Final R indices [I>2sigma(I)]	R1 = 0.0356, wR2 = 0.0870	R1 = 0.0235, wR2 = 0.0539	R_1 = 0.0619, wR_2 = 0.1714	R1 = 0.0366, wR2 = 0.0782	R_1 = 0.1095, wR_2 = 0.3157
R indices (all data)	R1 = 0.0441, wR2 = 0.0917	R1 = 0.0252, wR2 = 0.0547	R_1 = 0.0883, wR_2 = 0.2281	R1 = 0.0563, wR2 = 0.0866	R_1 = 0.1162, wR_2 = 0.3456
Absolute structure parameter	0.002(8)	0.010(5)	-0.03(5)	0.032(10)	-0.07(8)

Single crystal X-ray diffraction measurements revealed that ((*R)*-(+)-napthyl-1-ethylammonium tetrachlorocuprate (II) – (**3**) and ((*R)*-(+)-napthyl-2-ethylammonium tetrachlorocuprate (II)-(**4**) crystallizes into monoclinic crystal system with non centrosymmetric space group $P2_1$ and C_2 with unit cell parameters a = 12.7159(4), b = 7.1977 (2), c = 14.0548(4) Å and a = 10.7967(3), b = 7.2349(2), c = 16.9456(4) Å with Z = 2 at 296K, respectively. The structure of **3** and **4** consists of discrete naphthyl ethylammonium cations and $CuCl_4^{2-}$ anion as shown in Figure 6.7.

In compound **3**, $[CuCl_4]^{2-}$ anion exist in an isolated and highly distorted tetrahedral geometry with *trans* angles 138.70 and 145.17º and average *cis* angles of 97.21º and 94.89º**.** The observed yellow color of compound **3** is consistent with the value of the *trans* angle [20]. The deformation from tetrahedral geometry can be expressed by the dihedral angle between (Cl (l)-Cu-Cl (4))-(Cl (2)-Cu-C1 (3)) of 52.22º. The $[CuCl_4]^{2-}$ anion in **4** (green color) also shows isolated tetrahedral geometry (in between of square planar and tetrahedral geometry) with *tran*s angle of 153.90º and average cis angles of 91.97º and 93.84º [21]. Crystal structure of **3** (2.235 and 2.260Å) and **4** (2.230 and 2.259Å) showed similar bond length of $CuCl_4^{2-}$ ions. Tetrahedral geometry deformation [(Cl (l)-Cu-Cl (4))-(Cl (2)-Cu-Cl (3))] is much smaller in **4** (36.31º) as compared to deformation in **3**. The copper atoms lay on C_2 symmetry sites in both structures. In **3**, the distance between adjacent copper atoms (stacked) along crystallographic *a*-axis is 7.198Å while interlayer distance between copper atoms (stacked) along crystallographic *b*-axis is 14.055Å. On the other hand, for **4** adjacent (stacked) copper atoms distance along crystallographic *a*-axis are 6.498Å apart while 16.946Å along crystallographic *b*-axis.

In both compounds, asymmetric unit showed two naphthalene molecules but with slight difference in their planarity. This difference is 2.20º and 0.75º in asymmetric unit of **3** while it is 0.56º and 0.35º in asymmetric unit of **4**. This is reflected in observed NH···Cl hydrogen bonding pattern for two ligands in a same compound/molecule with different synthon's A and D. In **3** one of the naphthalene ammonium cation shows two hydrogen bonds (motif 1) whiles other which dissects the plane with former naphthalene ring at 10.70º, showed three hydrogen bonds (motif 2). Therefore $[CuCl_4]^{2-}$ anion in **3** shows one N–H···Cl hydrogen bond (3.294Å) and two bifurcated 2(N–H)···Cl hydrogen bonds with

dissimilar distances (3.197 and 3.248Å; 3.136 and 3.277Å). On the contrary both naphthalene ammonium cations in **4** interacts with three anions via two N–H···Cl hydrogen bonds (both 3.169Å) and two asymmetrically bifurcated 2(N–H)···Cl hydrogen bonds (3.208 and 3.247Å) (motif 3).

We also observed supramolecular interactions in the form of C-H···π interaction in **3** (C5(#1)-H···C8; 2.852Å) and **4** (C6(#1)-H···C8; 2.833Å) between two stacked layers naphthalene ligand, along crystallographic *a*-axis.

6.5.2 Crystal structure of 3 at 150K (3LT) and 350K (3HT)

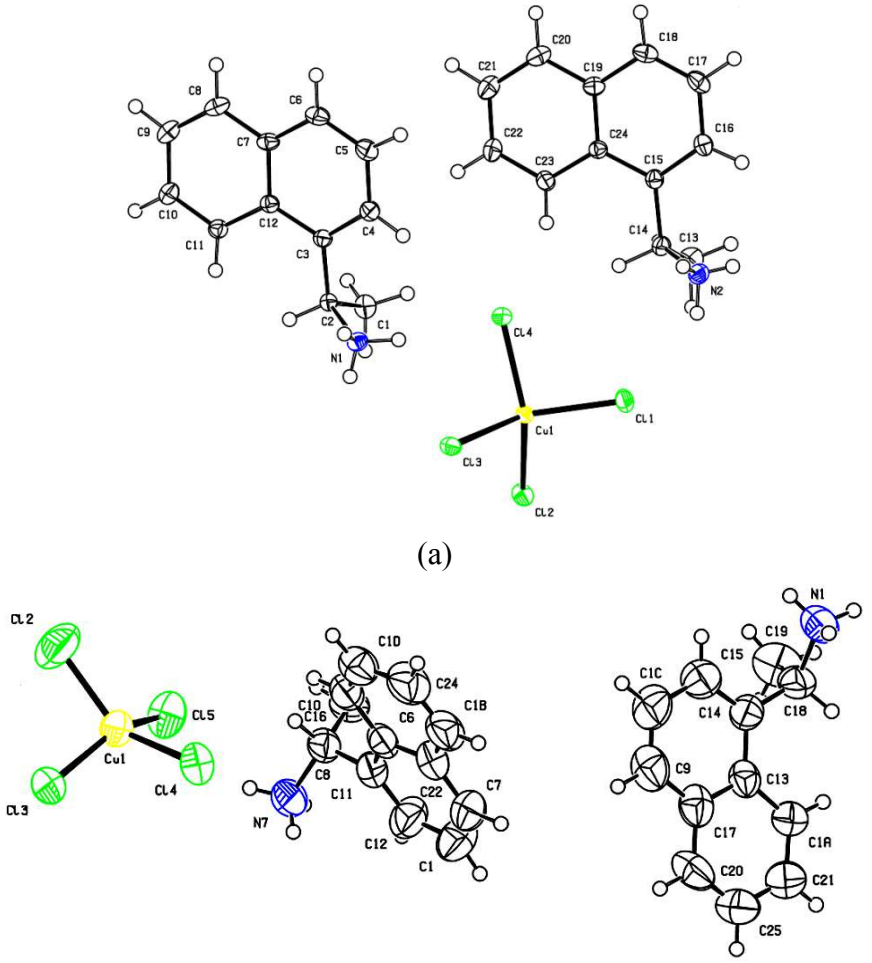

Fig. 6.8: View of the copper (II) coordination sphere in (a) 3LT; (b) 3HT

The X-ray crystal structure of ((*R*)-(+)-napthyl-1-ethylammonium tetrachlorocuprate (II) at 350K (**3HT**) and 150K (**3LT**) is monoclinic, $P2_1$ space group with Z = 2 (Figure 6.8-a,b). The observed change in crystal volume (**1**-1282.63(7) Å^3; **3LT**-1256.43(3) Å^3; **3HT**-1294.40 Å^3) near phase transition temperatures is negligible. At **3HT** *trans* angles are of 139.25 and 144.94º and average *cis* angles are of 97.17º and 94.85º while in **3LT** *trans* angles of 139.13 and 144.73º 94º with average *cis* angles of 97.16º and 95.01º. Cu-Cl bond lengths in $CuCl_4^{2-}$ ions for **3HT** and **3LT** remain quite similar (average bond lengths 2.238Å and 2.259Å for **3HT**; 2.216Å and 2.248Å for **3LT**). This confirms that at phase transition temperature and during thermochromic behavior $[CuCl_4]^{2-}$ anion has no direct role. All chloride atoms of $[CuCl_4]^{2-}$ anion in **3LT** involved in Cl···N interaction and follow synthon B and motif 3 for stabilization of distorted geometry, as shown in Figure 6.9. This is not the case with **3HT**, where motif 1 dictates stabilization [22].

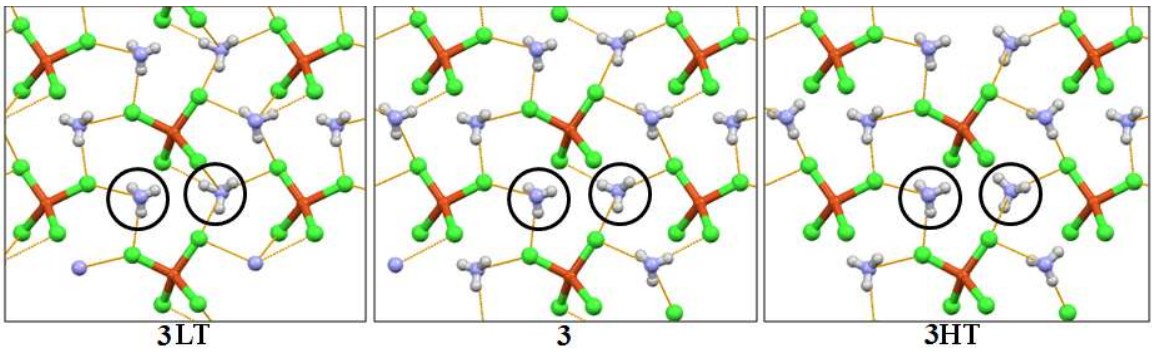

Fig. 6.9: Hydrogen bonding pattern of compound 3 at different temperature. (N–H---Cl hydrogen-bonded supramolecular motif)

3LT shows $[CuCl_4]^{2-}$ anion with one N–H···Cl hydrogen bond (3.294Å) and one bifurcated N–H···Cl hydrogen bond (3.131 and 3.263Å). While remaining two chloride atoms of $[CuCl_4]^{2-}$ anion follow synthon A, [N–H···2Cl; (3.264 and 3.275Å)]. Interestingly, in **3LT**, two neighboring ammonium cations show distinctly different hydrogen bonding motif, one with four while other with two hydrogen bonds, as shown in Figure 6.9.

This might be the reason for dissimilarity of two naphthalene (ligand) molecules planarity in a same asymmetric unit. The difference in planarity for **3HT** (2.25º and 0.56º) and **3LT** (2.59º and 0.51º). This is reflected in change in supramolecular interactions in the

form of C-H···π interaction in **3HT** (C5(#1)-H···C8; 2.851Å) as compared to **3LT** (C12(#1)-H···C3(#2) (3.314Å)) between two stacked layers of naphthalene ligand (Figure 6.10).

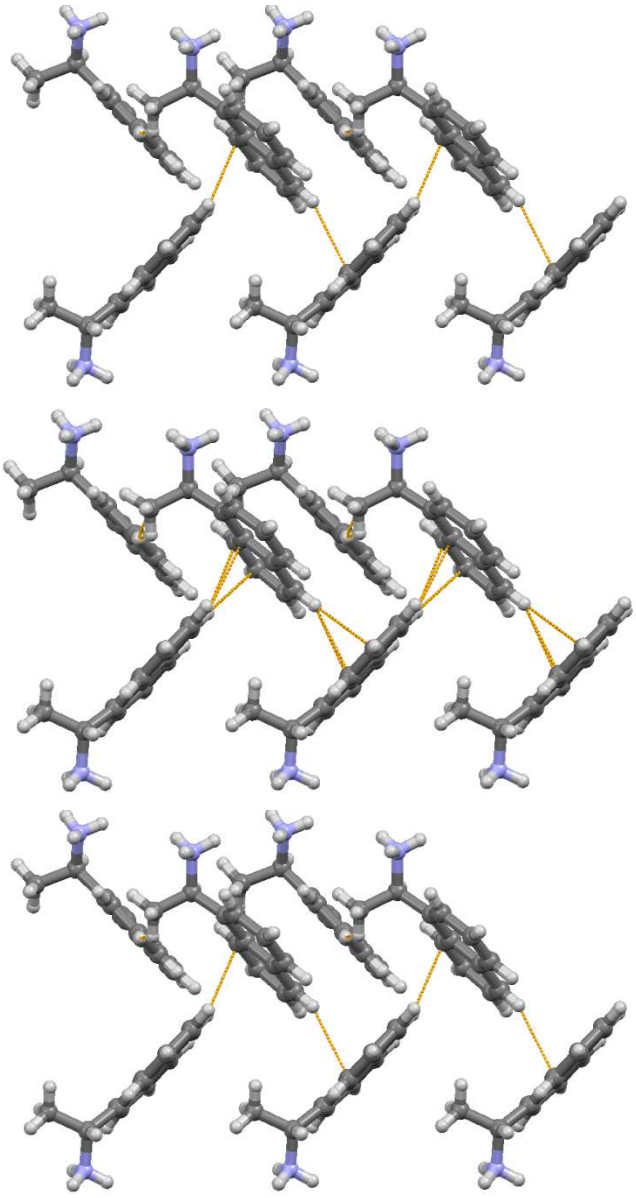

Fig. 6.10: Supramolecular C-H…π interactions in 3 present along the ligands

Selected bond length, bond angles and hydrogen bonds are listed in Table 6.3 and 6.4.

6.5.3 Crystal structure of 4 at 296K and 397K

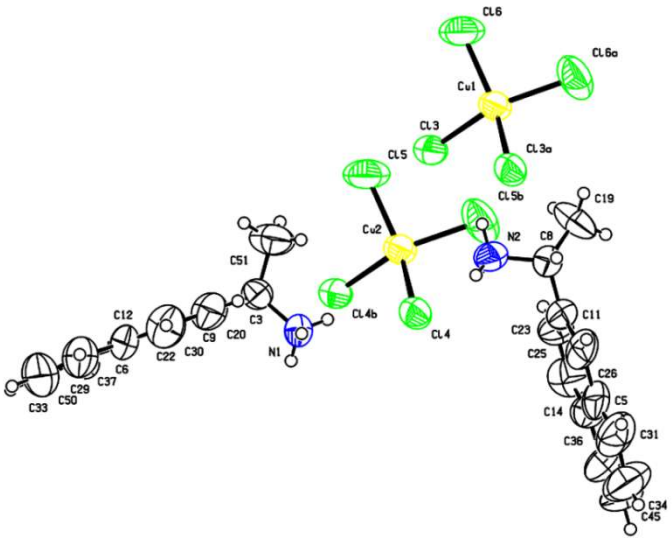

Fig. 6.11: View of the copper (II) coordination sphere in 4HT. Thermal ellipsoids are drawn at 50% probability

Crystal structure of ((*R)*-(+)-napthyl-2-ethylammonium tetrachlorocuprate (II) at 397K (**4HT**) is monoclinic, $P2_1$ with Z=2 (Figure 6.11).

The $[CuCl_4]^{2-}$ anion geometry in **4HT** at phase transition temperature does not showed much difference in *tran*s angle (153.59º) and in average cis angles (91.98º and 93.96º) compared to **2.** Cu-Cl bond lengths in $CuCl_4^{2-}$ ions for **4HT** and **4** remain quite similar (average bond lengths 2.2380 and 2.266Å for 2HT; 2.237 and 2.270(3) Å for 2). Tetrahedral geometry deformation [(Cl (l)-Cu-Cl (4))-(Cl (2)-Cu-Cl (3))] does not showed much change and remained smaller in **4HT** (36.64º). There is marginal increase in adjacent intralayer copper atom distances from 6.568Å to 7.263Å in **4HT**. These observations confirm the role of $CuCl_4^{2-}$ anion is restricted by rigid napthyl-2-ethylammonium ligand.

Each ammonium cation in **4HT** interacts with three anions via two N–H···Cl hydrogen bonds (both 3.185Å) and two asymmetrically bifurcated 2(N–H)···Cl hydrogen bonds ((3.229Å and 3.253Å) (synthon B, motif 3)). In **4** and **4HT (**0.45º), angle between planes of two benzene rings of naphthalene ring are almost planar.

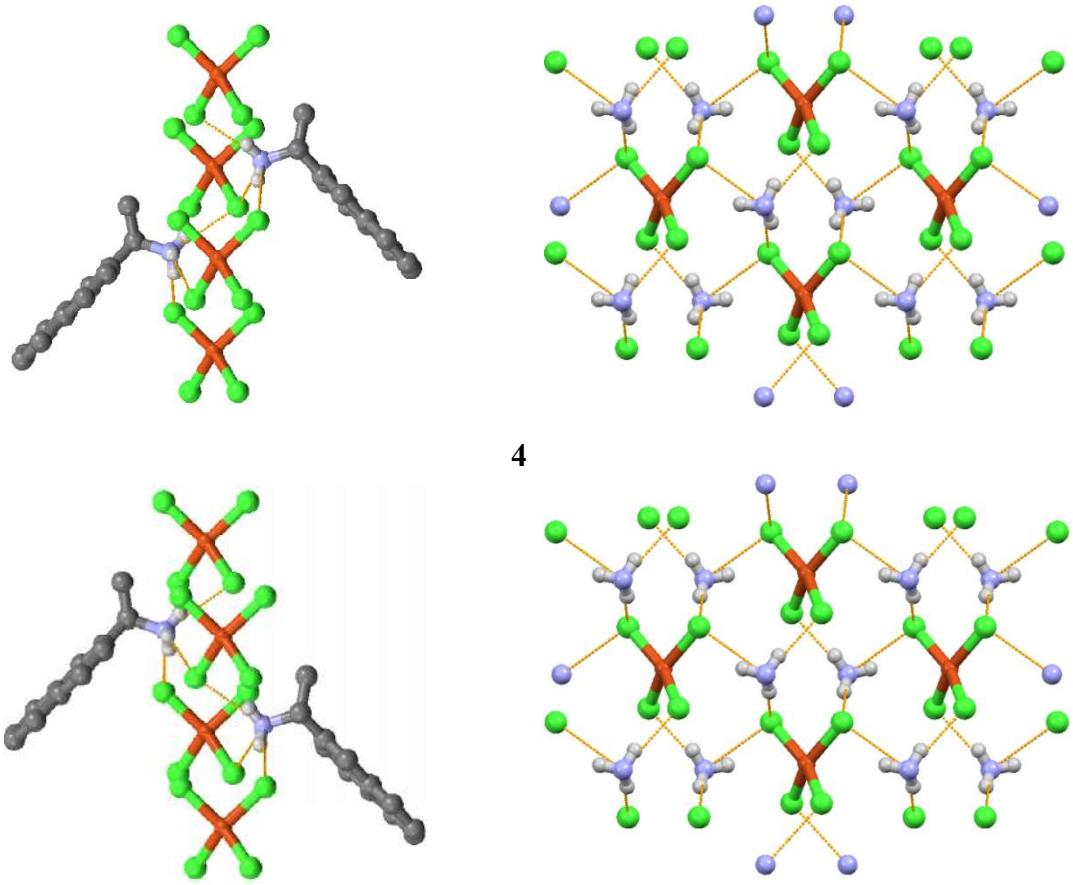

Fig. 6.12: Hydrogen bonding pattern of compound 4 at different temperature

In **4HT**, all ligands are parallel to each other forming layer surprisingly similar to **4** with same hydrogen bonding pattern (Figure 6.12) but with distinct change in colour of the crystal. These results are differing with **1** and **1HT** in which change in hydrogen bonding pattern causes color change.

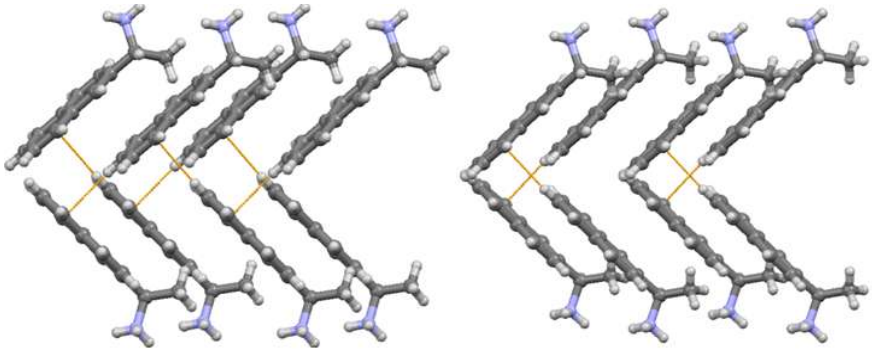

Fig. 6.13: Supramolecular C-H···π interactions in 4 (continuous) and 4HT (non-continuous) present along the ligands

This made us to look closely supramolecular interactions (C-H···π), which become weaker in **4HT** (as compared to **4)** between two stacked layers of naphthalene ring (C6(#1)-H···C8; 2.910Å). Supramolecular interactions are of continuous in nature for **4** while they are cross dimeric (non-continuous) nature in **4HT**, as shown in Figure 6.13.
This confirms that thermochromism observed in both compounds (**3** and **4**) does not occur due to change in $CuCl_4^{2-}$ ions geometry and is mostly due to alteration in ligand surrounding. No major phase or structural change involving the $CuCl_4^{2-}$ ion occurs in compound **3** and **4** and that the thermochromism is simply a result of the variation in band width. This same conclusion carries over to a number of other salts reported in literature [23].

The list of selected bond length, bond angles and hydrogen bonds are shown in Table 6.3 and 6.4.

Table 6.3: Selected bond lengths, bond angles and hydrogen bonds for 3, 3HT, 3LT, 4 and 4HT

Compounds	Cu-Cl Dist.	Cu-Cu Dist.[Å] Inter	Cu-Cu Dist.[Å] Intra	Cl-Cu-Cl Angle [º]	N-H···Cl Dist. [Å]	N-H···Cl Angle[°]
3	2.2397(4)	14.055	7.198	145.17(2)	3.294(2)	170(3)
	2.2578(3)		7.357	138.70(4)	3.197(2)	152(2)
	2.2610(3)			97.74(3)	3.249(2)	154(2)
	2.2372(3)			96.66(2)	3.277(2)	147(3)
				95.22(3)	3.3559(19)	118(2)
				94.56(2)	3.343(2)	159(3)
					3.136(2)	165(3)
3HT	2.216(4)	14.094	7.211	144.93(12)	3.267(3)	141.63(2)
	2.215(3)		7.294	139.25(18)	3.143(4)	164.19(3)
	2.243(3)			98.03(18)	3.242(2)	152.94 (2)
	2.255(4)			94.62(13)	3.183(2)	150.28(2)
				95.07(12)		
				96.32(11)		
3LT	2.2397(4)	13.972	7.156	144.731(13)	3.2746(11)	115.2(15)
	2.2578(3)		7.208	139.132(18)	3.2637(11)	159.6(17)
	2.2610(3)			97.547(15)	3.1962(12)	154.4(13)
	2.2372(3)			96.680(12)	3.2220(12)	155.8(17)
				95.220(14)	3.3184(13)	170.0(19)
				94.801(13)	3.1306(14)	166.4(17)
					3.2630(13)	142.9(16)
					3.3298(12)	120.5(14)
4	2.2295(6)	16.946	6.498	153.90(3)	3.4839(17)	129.0
	2.2592(5)		7.235	153.90(3)	3.2085(15)	153.8
				95.16(4)	3.1692(19)	156.2
				92.52(2)	3.2470(17)	136.3
				92.52(2)	3.5427(18)	146.4
				91.42(3)		
4HT	2.266(3)	17.014	6.568	153.66(17)	3.224	160.36
	2.238(4)		7.263	153.59(17)	3.246	145.34
	2.270(3)			91.61(18)	3.229	160.22
	2.245(4)			95.1(3)	3.185	162.25
				91.39(18)	3.229	160.22
				92.59(13)	3.253	141.91
				95.3(3)		

.

Table 6.4. Interatomic distances (Å) of ligand hydrochlorides in all compounds

Atom	Atom	3 Length/Å	3HT Length/Å	3LT Length/Å	4 Length/Å	4HT Length/Å
First Ligand hydrochloride _RNH_3						
C1	C2	1.377	1.365	1.381	1.364	1.379
C2	C3	1.410	1.430	1.409	1.421	1.423
C3	C4	1.355	1.323	1.367	1.359	1.391
C5	C6	1.351	1.376	1.370	1.345	1.352
C6	C7	1.404	1.373	1.404	1.389	1.423
C7	C8	1.375	1.345	1.374	1.352	1.401
C8	C9	1.418	1.413	1.424	1.393	1.366
C9	C10	1.423	1.403	1.422	1.414	1.407
C9	C1	1.432	1.432	1.436	1.425	1.416
C10	C4	1.406	1.414	1.417	1.395	1.327
C10	C5	1.427	1.410	1.418	1.450	1.468
C1	C11	1.507	1.503	1.506	1.509	1.530
C11	C12	1.509	1.497	1.515	1.511	1.522
C11	N1	1.503	1.523	1.504	1.503	1.484
Second Ligand hydrochloride _RNH_3						
C1	C2	1.375	1.356	1.379	1.364	1.401
C2	C3	1.401	1.426	1.411	1.421	1.391
C3	C4	1.359	1.331	1.364	1.359	1.353
C5	C6	1.360	1.353	1.374	1.345	1.410
C6	C7	1.394	1.388	1.402	1.389	1.383
C7	C8	1.375	1.339	1.375	1.352	1.331
C8	C9	1.423	1.426	1.424	1.393	1.366
C9	C10	1.421	1.391	1.418	1.414	1.428
C9	C1	1.432	1.453	1.435	1.425	1.445
C10	C4	1.414	1.411	1.420	1.395	1.355
C10	C5	1.418	1.411	1.422	1.450	1.484
C1	C11	1.510	1.497	1.507	1.509	1.512
C11	C12	1.511	1.531	1.519	1.511	1.500
C11	N1	1.498	1.524	1.502	1.503	1.504

CCDC No. 916611 and 916612 contains the crystallographic data for the compounds **3** and **4** respectively. These data can be obtained free of charge via http://www.ccdc.cam.ac.uk/conts/retrieving.html,or from the Cambridge Crystallographic Data Centre, 12 Union Road, Cambridge CB2 1EZ, UK; fax: (+44) 1223 336 033; or e-mail: deposit@ccdc.cam.ac.uk.

6.6 Variable temperature FT-IR

Variable temperature analysis on compound **3** (Figure 6.14) in KBr pellet showed that at phase transition temperature i.e. in **3HT** (347K), stretching vibration mode of NH_3^+ (**3099, 3049 and 3019 cm^{-1}**) gets merged, increased in absorbance and form a single band (3037 cm^{-1}), in accordance with single crystal XRD studies where rearrangement of hydrogen bonding is observed near phase transition temperature. It is further supported by a shift in the bending modes of N-H (1596 → 1589 cm^{-1}) and deformation mode shift (1059→1056 cm^{-1}). Phase transition resulted in decrease in hydrogen bonding of amino cation and hence increase in absorbance of NH_3^+ and decrease in asymmetric stretching of $-CH_3$ (2925). Latter effect is also observed in single crystal structure where C-H---π interaction between methyl proton get diminished at HT. The C-H vibrations of the ligand molecule for **3** also shift from 1485→1479 cm^{-1} and from 1137→1132 cm^{-1}. The observed doublet band at 911 and 906 cm^{-1} decreased and merged into a new single band at 909 cm^{-1}. Broad band at 604 gets sharp at high temperature with generation of 594 cm^{-1} band. New band appeared at 667 cm^{-1} at a phase transition temperature. The origin of this band was unknown in **3**. The band at 957 cm^{-1} for C-H wagging in **3** gets disappeared with an increase in temperature.

Variable temperature analysis on compound **4** (Figure 6.15) at phase transition temperature i.e. in **4HT** (347K) showed opposite situation compared to **3HT**. Stretching vibration mode of NH_3^+ (**3101, 3057 and 3041 cm^{-1}**) gets merged and decresed in absorbance forming a single band (3053 cm^{-1}) while asymmetric stretching of terminal methyl gets increased and shifted by 15 cm^{-1} in accordance with single crystal XRD study where strong hydrogen bonding between the cation and the $CuCl_4^{2-}$anion is observed in high temperature phase i.e. **4HT**. The *in-plane* C-H deformation mode of **4** gets shifted from 1094→1087 cm^{-1} in **4HT**. The C-C stretching mode also get shifted from 1591→1586 cm^{-1}. Shifting in bands also observed for CCC bend (602→597 cm^{-1})and ring deformation (826→820 cm^{-1}) modes at HT.

All decreased, spilt and disappeared band shows reversibility while cooling in both compounds. These results indicate that the molecular rearrangement originated in ligand takes place in crystal packing at phase transition temperature.

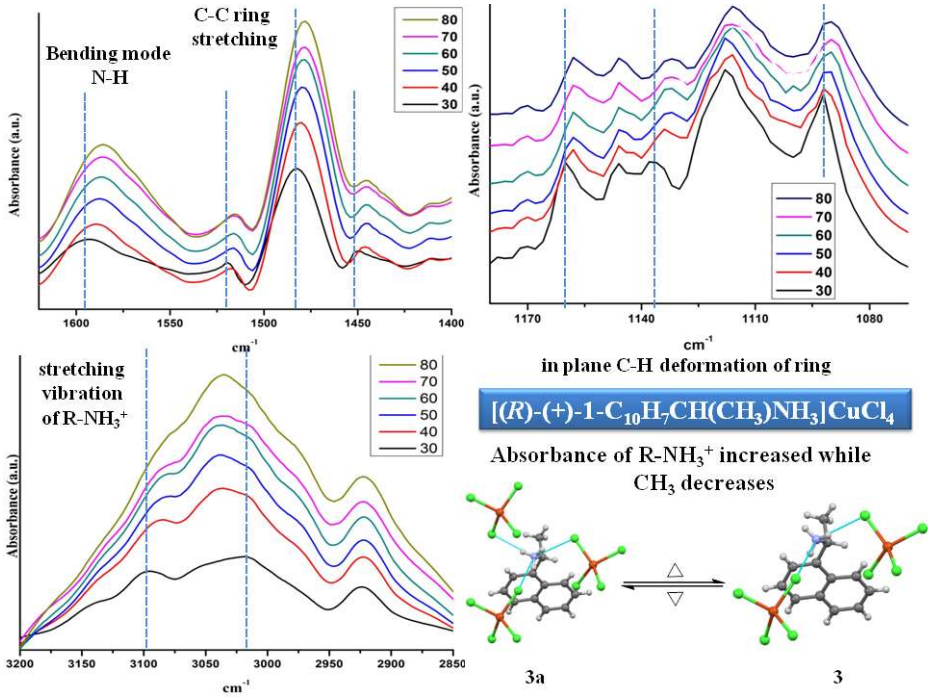

Fig. 6.14: Variable temperature FT-IR spectra of compound 3

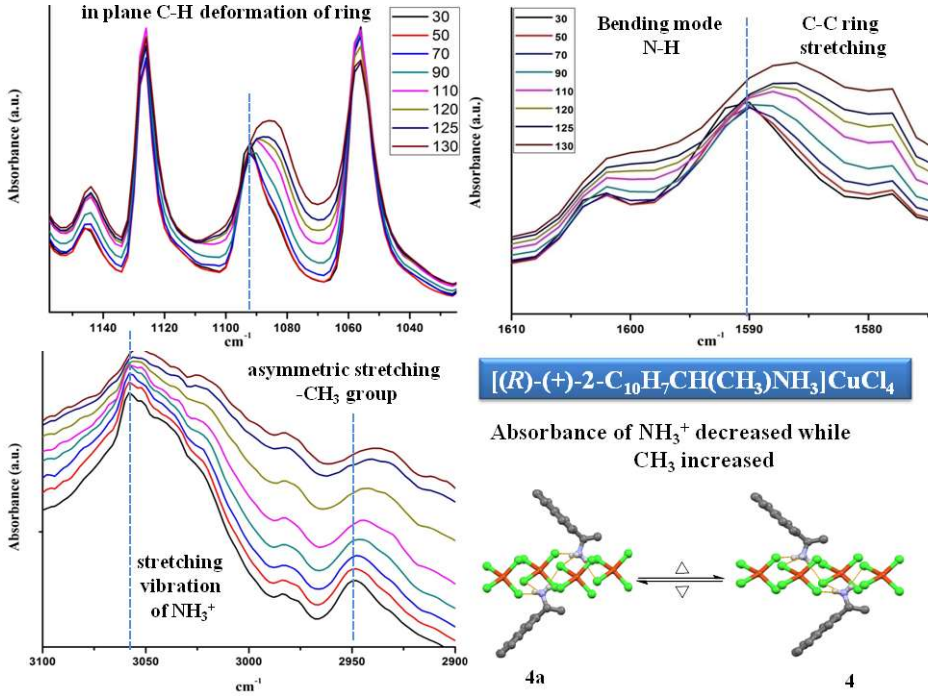

Fig. 6.15: Variable temperature FT-IR spectra of compound 4

6.7 Optical properties

6.7.1 UV Spectra:

(*R*)-(+)-napthyl-1-ethylamine hydrochloride, salt of **1 (1HCl),** showed absorbance maxima at 294 nm while its hybrid compound **3** showed a bathochromic shift (red shift) at 277nm. Compound 3 showed sign of d-d transition at 832 nm as shown in insight fig 6.16a. The position of the *d-d* band in **3** is very similar to that reported for the copper(II) complexes in which copper(II) atoms have a distorted tetrahedral-based geometry [24].

(*R*)-(+)-2-napthyl-1-ethylamine hydrochloride, salt of **2 (2HCl)**, showed absorbance maxima at 280 nm. Compound **4** does not show any bathchromic or hypsochromic shift and having absorbance maxima at 280 nm only. Compound **4** also showed sign of *d-d* transition at 689 nm due to quasi square planar geometry around $CuCl_4^{2-}$ dianion. (Figure 6.16b for insight).

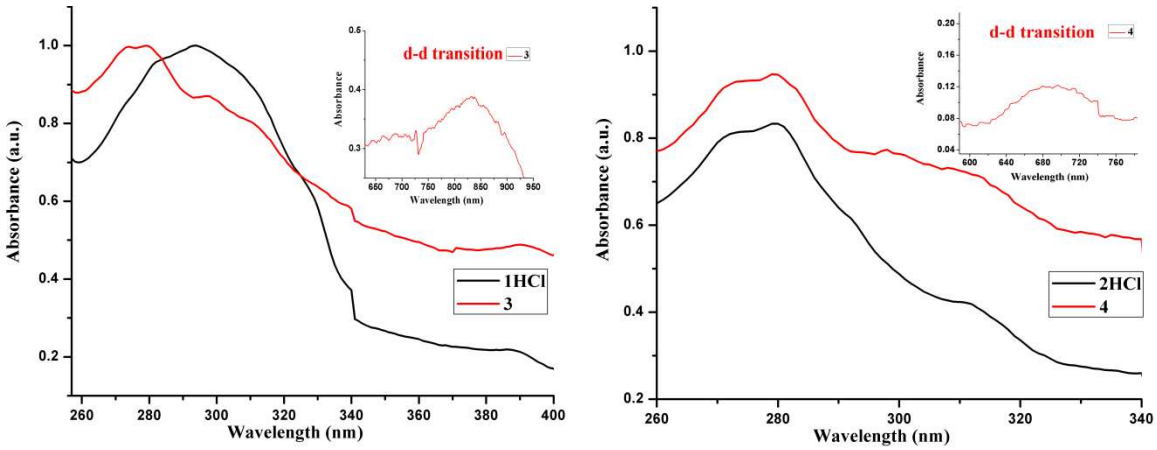

Fig. 6.16 (a, b): Showing the solid state electronic spectra of the ligand hydrochloride (1HCl and 2HCl) and compound 3 and 4 in nujol

6.7.2 Solid state fluorescence:

The photoluminescence spectra of ligand hydrochloride (**1HCl** and **2HCl**) and compound **3** and **4** were recorded on crystalline samples at room temperature.

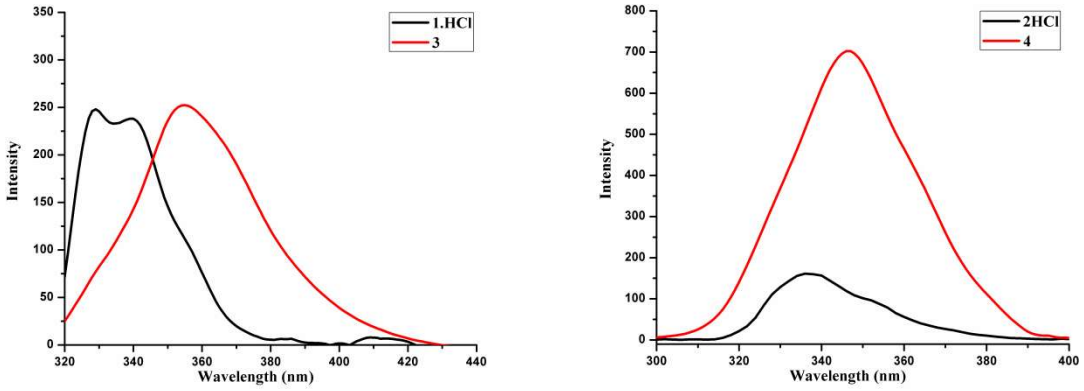

(a) **(b)**

Fig. 6.17(a, b): Solid state fluorescence behavior of ligand hydrochloride (1HCl and 2HCl) and compound 3 and 4 in nujol

Compound **1HCl** showed fluorescence maxima (Figure 6.17a) at 329 nm and 339 nm (excitation wavelength: 294 nm). Compound **3** (excitation wavelength : 277nm) showed slight hypsochromic emission spectra with maxima at 354nm. This emission observed can be considered ligand hydrochloride centric in nature. Compound **3** shows slightly high intensity in fluorescence than hydrochloride salt (**1HCl**). Reason behind this is in the crystal structure of **1HCl** and **3** at 296K**.** The angle between the two planes passing through benzene rings of naphthalene makes the angle of 3.00º and 2.20º, 0.75º . In crystal structure **3HT** at 350K showed the angle between two planes passing through a benzene rings of naphthalene ring gives 2.59º and 0.51º which will decrease the emission intensity as compared to an intensity of **3**.

Compound **2HCl** showed fluorescence maxima (excitation wavelength: 280 nm) at 336 nm (Figure 6.17b). While compound **4** (excitation wavelength: 280 nm) showed slightly red shifted fluorescence maxima at 346 nm. Distinctly observed change in fluorescence intensity can be compared to the planarity of the ligand molecules. In compound **2HCl,** planes passing through naphthalene ring makes an angle of 1.48º, which is higher than **4.** In **4** this angle is 0.35, that means it is nearly in same plane. Interestingly, **4HT** at 397K showed angle 1.26º will surely show decrese in fluorescence intensity.

Observed enhancement and red shift in the emission spectra of both compounds **3** and **4** in solid state attributed to presence of planar naphthalene ring as compared to their **1HCl** and **2HCl** salts. Hence one can monitor the structural phase transition due to change in temperature by emission behavior originated in ligand itself.

6.8 Conclusion

- Synthesized and characterized two copper based compounds **3** and **4** using FT-IR, CHN and single crystal X-ray diffraction.
- Compounds were investigated for structural phase transitions using TG/DTA, DSC, single crystal XRD and Variable Temperature IR.
- TG-DTA showed endothermic transition, with possibility of solid-solid structural phase transition. DSC measurements showed 'reversible' nature of these transition for both the compounds in the range of 350-371K.
- Single crystal X-ray studies on both the compounds showed $CuCl_4^{2-}$ dianion remain in distorted tetrahedral geometry irrespective of change in temperature. There in also no observable change in Cl-Cu-Cl bond length and angles.
- Distinct synthons in the form of NH···Cl hydrogen bonding are observed in both the compounds. These synthons form different motifs with change in temperature.
- Different Hydrogen bonding pattern between two ligand molecules attached to same center leads to thermochromic and fluorescence behavior.
- Thermochromism in compounds can be tuned at molecular level using proper NH---Cl synthons or motifs, and should not be confined to geometry change around metal polyhedra.
- Thermochromism is not thought to result from a gross geometry change of the Cu-(II) chromophores, but rather a variation of the ligand field strength due to a change in the (*R)*-(+)-napthyl-1-ethylamine and (*R)*-(+)-2-napthyl-1-ethylamine conformation with temperature.

6.9 References:

[1] J. H. Day, *Chem. Rev.* **1963**, *63*, 65-80.

[2] D. R. Bloomquist, R. D. Willett, *Coord. Chem. Rev* **1982**, *47*, 125-164.

[3] (a) C. Pariya, F.-L. Liao, S.-L. Wang, C.-S. Chung, *Polyhedron* **1998**, *17*, 547-554; (b) R. Bhattacharya, M. Sinha Ray, R. Dey, L. Righi, G. Bocelli, A. Ghosh, *Polyhedron* **2002**, *21*, 2561-2565; (c) M. Kronstein, K. Kriechbaum, J. Akbarzadeh, H. Peterlik,M.- A. Neouze, *Phys. Chem. Chem. Phys.* **2013**, *15*, 12717-12723; (d) U. El-Ayaan, F. Murata, Y. Fukuda, *Monatsh. Chem. /Chemical Monthly* **2001**, *132*,1279-1294.

[4] (a)H. Hardt, A. Pierre, *Z. Anorg. Allg. Chem.* **1973**,*402*,107-112. (b) H. D. Hardt, A. Pierre, *Inorg. Chim. Acta* **1977**, *25*, L59-L60.

[5] (a) D. R. Bloomquist, R. D. Willett, H. W. Dodgen, *J. Am. Chem. Soc.* **1981**, *103*, 2610-2615; (b) S. Roberts, D. Bloomquist, R. Willett, H. Dodgen, *J. Am. Chem. Soc* **1981**, *103*, 2603-2610; (c) D. R. Bloomquist, R. D. Willett, *J. Am. Chem. Soc* **1981**, *103*, 2615-2619.

[6] (a) D. Partlow, S. Gurkovich, K. Radford, L. Denes, *J. Appl. Phys.* **1991**, *70*, 443-452; (b) P. Kiri, G. Hyett, R. Binions, *Adv. Mater. Lett.* **2010**, *1*, 86-105.

[7] L. Suchow, P. H. Keck, *J. Am. Chem. Soc.* **1953**, *75*, 518-522.

[8] M. Seredyuk, A. B. Gaspar, V. Ksenofontov, S. Reiman, Y. Galyametdinov, W. Haase, E. Rentschler, P. Gütlich, *Chem. Mater.* **2006**, *18*, 2513-2519.

[9] H. Xie, S. O'Dwyer, J. Corish, D. Morton-Blake, *Synth.Met.* **2001**, *122*, 287-296.

[10] A. Seeboth, D. Lötzsch, E. Potechius, R. Vetter, *Chin. J. Polym. Sci.* **2006**, *24*, 363-368.

[11] J. G. Hughes, *J. Chem. Educ.* **1998**, *75*, 57.

[12] (a) D. R. Bloomquist, M. R. Pressprich, R. D. Willett, *J. Am. Chem. Soc.* **1988**, *110*, 7391-7398 (b) M. J. Riley, D. Neill, P. V. Bernhardt, K. A. Byriel, C. H. Kennard, *Inorg. Chem.* **1998**, *37*, 3635-3639 (c) A. O. Polyakov, A. H. Arkenbout, J. Baas, G. R. Blake, A. Meetsma, A. Caretta, P. H. van Loosdrecht, T. T. Palstra, *Chem. Mater.* **2011**, *24*, 133-139.

[13] C. Zanchini, R. D. Willett, *Inorg. Chem.* **1990**, *29*, 3027-3030.

[14] (a) R. Harlow, W. J. Wells III, G. W. Watt, S. Simonsen, *Inorg. Chem.* **1974**, *13*, 2106-2111; (b) M. Udupa, B. Krebs, *Inorg. Chim. Acta* **1979**, *33*, 241-244; (c) H. C. Nelson, S. H. Simonsen, G. W. Watt, *J. Chem. Soc., Chem. Commun.* **1979**, 632-633; (d) L. Antolini, A. Benedetti, A. Fabretti, A. Giusti, *Inorg. Chem.* **1988**, *27*, 2192-2194; (e) M. J. Riley, D. Neill, P. V. Bernhardt, K. A. Byriel, C. H. Kennard, *Inorg. Chem.* **1998**, *37*, 3635-3639.

[15] S. Haddad, R. D. Willett, *Inorg. Chem.* **2001**, *40*, 2457-2460.

[16] G. R. Desiraju, *Angew. Chem. Int. Ed.* **1995**, *34*, 2311-2327.

[17] C. J. Adams, H. M. Colquhoun, P. C. Crawford, M. Lusi, A. G. Orpen, *Angew. Chem. Int. Ed.* **2007**, *46*, 1124-1128.

[18] B. Dolling, A. L. Gillon, A. G. Orpen, J. Starbuck, X.-M. Wang, *Chem. Commun.* **2001**, 567-568.

[19] A. Srivastava, V. Singh, *Indian J. Pure Appl. Phys.* **2007**, *45*, 714.

[20] C. Zanchini, R. D. Willett, *Inorg. Chem.* **1990**, *29*, 3027-3030.

[21] L. Battaglia, A. Bonamartini Corradi, G. Marcotrigiano, L. Menabue, G. Pellacani, *Inorg. Chem.* **1979**, *18*, 148-152.

[22] R. Clay, P. Murray-Rust, J. Murray-Rust, J. Chem. Soc., Dalton Trans. **1973**, 595-599.

[23] R. Willett, J. Haugen, J. Lebsack, J. Morrey, *Inorg. Chem.* **1974**, *13*, 2510-2513.

[24] W. E. Hatfield, H. D. Bedon, S. M. Horner, *Inorg. Chem.* **1965**, *4*, 1181-1184.